Surface radiation budget at Thule, Greenland: role of clouds and surface albedo

D. Meloni[1], A. di Sarra[1], G. Pace[1], T. Di Iorio[1], M. Cacciani[2]
G. Mevi[2,3,a], G. Muscari[3]

[1]*Laboratory for Observations and Analyses of Earth and Climate, ENEA, Italy, e-mail: daniela.meloni@enea.it;*
[2]*Physics Department, University of Rome "La Sapienza", Italy;* [3]*Istituto Nazionale di Geofisica e Vulcanologia, Italy;* [a]*now at SERCO, Italy*

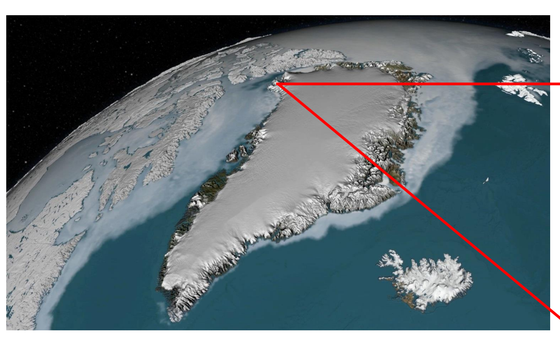

***The THAAO Observatory at Thule Air Base* (76.5°N, 68.8°W)**

Visit **http://www.thuleatmos-it.it**

Upward-looking radiometers

Downward-looking radiometers

HATPRO microwave profiler

Lidar

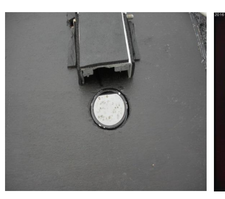

KT II-85 pyrometer

All Sky Cam image

Radiosounding

Introduction

The radiative balance of the Earth-atmosphere system is the driving motor of climate change, and polar regions are the most sensitive, at global level, to such changes. Among different factors, water vapour, clouds and the surface albedo have the most important influence on surface radiative budget (SRB) in the polar regions, acting with complex feedback mechanisms. The determination of cloud properties from satellite is problematic, thus requiring either long term measurements or intensive field campaigns.

The Thule High Arctic Atmospheric Observatory, THAAO, at Thule Air Base (76.5°N, 68.8°W), Greenland, is devoted to climate change studies since the 90's, with an international effort of different institutions, DMI, NCAR, ENEA, INGV, University of Rome and Florence, in the framework of the Network for the Detection of Atmospheric Composition Change (NDACC).

Instruments

The instruments available for the measurements of the SRB are pyranometers and pyrgeometers for the shortwave (SW) and longwave (LW) irradiances [1]: measurements of the downward components started in 2009, those for the upward component in 2016.

Other available instruments useful for the analysis of atmospheric properties are:

- a lidar system for stratospheric temperature and tropospheric aerosol [2,3,4];
- a microwave radiometer for the integrated water vapour (IWV), the liquid water path (LWP), and the temperature and relative humidity tropospheric profiles;
- VESPA-22 microwave spectrometer [5] for the water vapour stratospheric profiles and IWV;
- an infrared (9.6-11.5 μm) pyrometer for the sky brightness temperature (BT);
- a visible and an infrared sky cameras for the cloud cover;
- a meteorological station.

Moreover, a Vaisala radiosounding system is available during field campaigns.

SW and LW radiative budget and surface albedo

Measurements of SW and LW irradiances from July 2016 to September 2018 are considered here.

The pyranometer measurements have been corrected for the thermal offset of the instrument. For all the radiometers the most recent calibration and a correction accounting for the thermal dependence of the sensitivity have been applied.

Figure 1 presents the time evolution of the daily averaged downward and upward SW irradiances, and the derived daily SW albedo in the period from 14 July 2016 (when upward irradiance measurements started) to 31 December 2017.

Similarly, Figure 2 shows the time series of the daily averaged downward and upward LW irradiance, with the zenith sky brightness temperature in the 9.6-11.5 μm interval.

The SW and LW net irradiances have been calculated and the total (SW+LW) SRB have been computed (Figure 3).

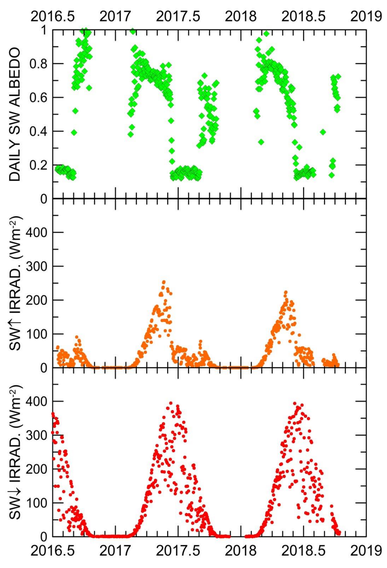

Figure 1: From top to bottom: time series of daily SW surface albedo, upward and downward SW irradiance

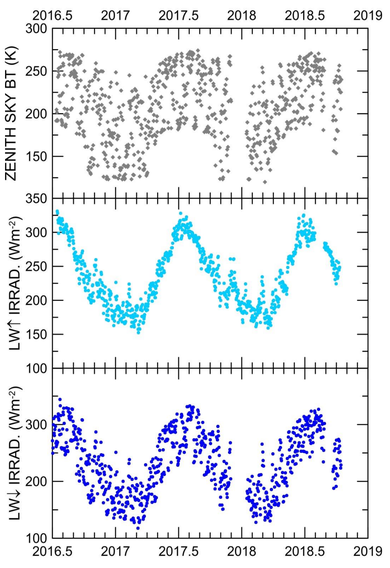

Figure 2: From top to bottom: time series of daily zenith sky brightness temperature (9.6-11.5 μm), upward and downward LW irradiance

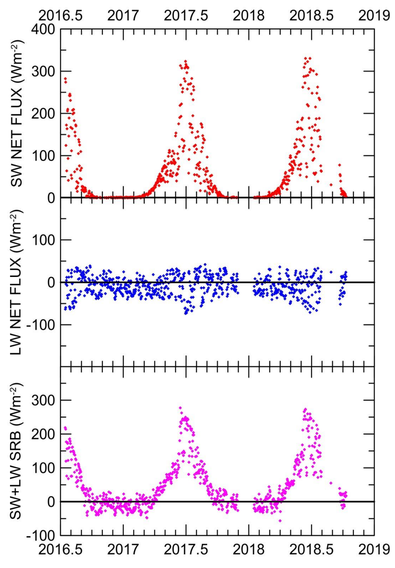

Figure 3: From top to bottom: time series of daily SW and LW net fluxes, and total (SW+LW) SRB

The surface SW albedo shows a clear annual behaviour, with values below 0.2 (average value 0.16) in the months with snow-free surface, typically June, July, and August, and values above 0.7 from March to April due to the reflection caused by the snow-covered surfaces, as evidenced by the reflected SW irradiance (Figure 1); intermediate values are found in June and September. It is worth noting that the albedo determination is not possible for the months when solar radiation is very low or completely absent.

Both components of the LW irradiance have a clear annual cycle, with maxima in summer and minima in winter. The larger variability of the downward component is associated to the cloud presence.

The SRB is driven by the LW radiation in winter and by the SW radiation in the rest of the year. In summer the LW component offsets the SW one by about 50 Wm^{-2}, i.e. by 17% at the peak.

Cloud radiative forcing

The measurements collected during the summer campaign of the Study of the water Vapour in the polar AtmosPhere (SVAAP) project in July 2016 have been analysed in order to derived an estimate of the cloud optical properties and of their radiative effect.

By parametrizing the SW and LW irradiances under cloud-free conditions, the surface cloud radiative forcing (CRF) can be calculated using the equation:

$CFR_{SW,\,LW} = Fnet_{SW,\,LW}\,(cloud) - Fnet_{SW,\,LW}\,(no\ cloud)$ where $Fnet = IRR\downarrow - IRR\uparrow$

The parametrized net fluxes are shown as black curves in Figure 4.

The cloud optical thickness (COT) can be derived following [6] from the downward SW irradiance and albedo, under the assumption of homogeneous cloud cover and no direct solar irradiance. Data for COT>10 in a time interval of 20 minutes have been selected in order to reduce the impact of broken clouds (Figure 5).

The cloud presence determines a decrease (increase) in SW (LW) irradiance, whereby changes depend on the cloud geometrical (base and top altitude), microphysical (phase, droplet effective radius, r_e), physical (LWP), and optical (COT) properties.

The LWP, filtered for values lower than 0.4 kg m^{-2} [7], has been used to retrieve r_e assuming that the liquid water content increases with altitude [8]:

$$r_e = \frac{9}{5}\frac{LWP}{COT\ \rho}$$ where ρ is the water vapour density.

The derived values of r_e (Figure 5) are generally below 20 μm. It should be taken into account that this methodology is based on the use of measurements from different instruments, thus requiring a careful data selection.

The retrieved surface CRF has been selected in a SZA interval of 60°±2.5°: the dependence on COT, LWP, r_e, and sky BT is plotted in Figure 6. The SW CRF has large negative values and a strong dependence on COT, while the LW CRF vary slightly for COT>20.

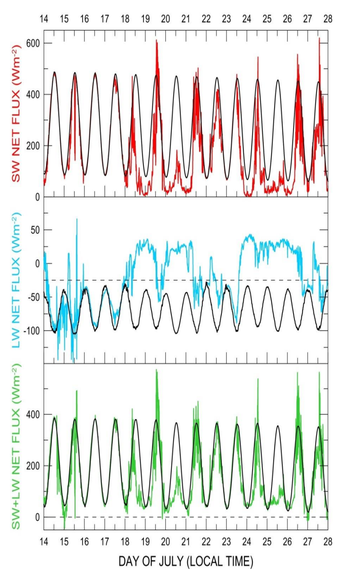

Figure 4: From top to bottom: time series of the SW, LW and total (SW+LW) surface net fluxes derived from measurements and from parametrizations for cloud-free conditions.

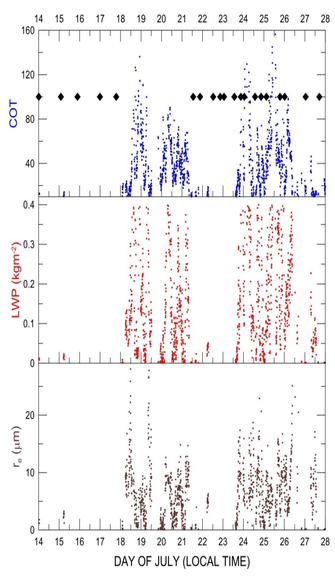

Figure 5: From top to bottom: time series of COT, LWP and re. Black diamonds represent the time of the radiosondes launches.

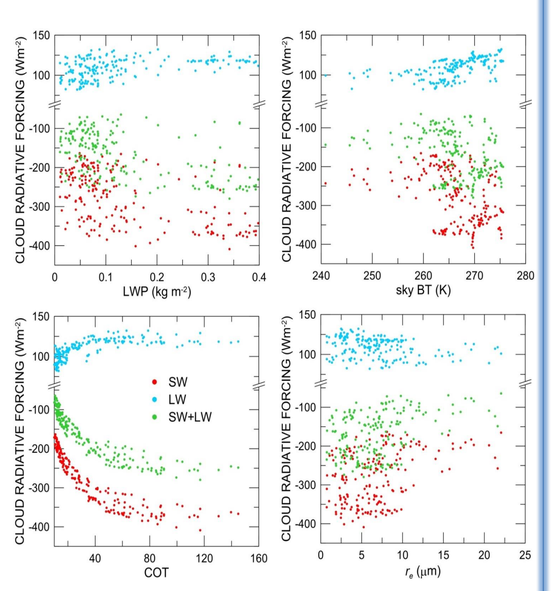

Figure 6: SW, LW and total surface CRF as a function of LWP, COT, sky BT, and r_e

References

1. Di Biagio, C., et al., 2012. Climate Dyn., 39, 953-969.
2. di Sarra A., et al., 1998. J. Geophys. Res., 103, doi:10.1029/98JD00901.
3. di Sarra, A., et al., 2002. J. Geophys. Res., 107(D12), 4152, doi:10.1029/2001JD001074.
4. Di Biagio, C., et al., 2010. J. Geophys. Res., 115, D24315, doi:10.1029/2010JD014070.
5. Bertagnolio, P. P., et al., 2012. Eur. J. Remote Sens., 45, 51-61, doi:10.5721/EuJRS20124506.
6. Barnard, J. C, and Long, C. N., 2004. J. Appl. Meteor., 43(7), 1057-1066.
7. Löhnert, U., and Crewell, S., 2003. Radio Sci., 38(3), 8041, doi:10.1029/2002RS002654.
8. Wood, R., and Hartmann, D. L., 2006. J. Climate, 19, doi:10.1175/JCLI3702.1.

Acknowledgements

Data used in this study have been collected under the SVAAP and OASIS-YOPP projects funded by the Italian Antarctic Programme (PNRA). This study has been also partially supported by Progetto Premiale ARCA.